

Iterative Deconvolution of Teleseismic P Waves from the Thessaloniki (N. Greece) Earthquake of June 20, 1978

GEORGIOS N. STAVRAKAKIS,¹ AKIS-G. TSELENTIS² and JOHN DRAKOPOULOS²

Abstract—Teleseismic long-period P waves from the June 20, 1978, Thessaloniki (N. Greece) earthquake ($M_s = 6.4$) were modeled in an attempt to extract information about asperities or barriers on the fault plane. The analysis is based on the inversion method of complex P waves developed by Kikuchi and Kanamori (1982). A far-field source time function with a rise time of 2 sec and a process time of 5 sec is inferred, corresponding to a source dimension of about 10 km when a rupture velocity of 2 km/sec is assumed.

The source depth of this shock, estimated by matching synthetic seismograms to observations, is found to be 8 km. The sum of the seismic moments of the individual subevents amounts to 3.3×10^{25} dyn-cm.

Key words: Deconvolution, teleseismic P waves, Thessaloniki (N. Greece).

1. Introduction

It is widely known that strong earthquakes often consist of a sequence of smaller multiple shocks (WYSS and BRUNE, 1967; KANAMORI and STEWART, 1978; KIKUCHI and SUDO, 1984; KIKUCHI and FUKAO, 1985).

The rupture complexity is a manifestation of a heterogeneous distribution of the mechanical properties along the fault and suggests the existence of relatively large, isolated, high-stress zones in the fault plane. The asperities or barriers are responsible for the rupture propagation (AKI, 1979; LAY *et al.* 1982). They are also responsible for the irregularity in the fault motion and thus control strong ground motions (MIKUMO and MIYATAKE, 1978; KANAMORI, 1982).

The purpose of this study is to understand better the detailed sequence of events during rupture associated with the Thessaloniki earthquake of June 20, 1978 ($M_s = 6.8$).

We applied the iterative-deconvolution method of complex P waves developed

¹ Earthquake Planning and Protection Organization, 196–198 Ippocratous Str., 11471 Athens, Greece.

² Department of Geophysics, University of Athens, Greece.

by KIKUCHI and KANAMORI (1982) and recently reaffirmed by KIKUCHI and SUDO (1984) and KIKUCHI and FUKAO (1985).

Nine WWSSN long-period seismograms are analysed, in the epicentral distance range of 45° to 85° , for information about the rupture propagation and the distribution of the asperities or barriers on the fault plane.

2. Iterative deconvolution of complex body waves

An earthquake source may be modeled as a series of double-couple point sources with the same focal mechanism (KIKUCHI and KANAMORI, 1982). Each point source is specified by the seismic moment m , the onset time s , and the coordinates (x, y) on the fault plane. In the following we take the x axis in the fault strike and the y axis in the dip direction. Hence, each individual subevent is specified by (m, s, x, y) , and a sequence of double-couple sources is given as

$$(m_i, s_i, x_i, y_i), \quad i = 1, 2, \dots \quad (1)$$

Let $w_j(t; x, y)$ denote a synthetic wavelet from a unit point source located at (x, y) on the fault plane, and let $X_j(t)$ denote the observed seismogram at the i^{th} station.

As the first step, the point source (m_i, s_i, x_i, y_i) is then determined, so that the residual error,

$$\Delta = \sum_{j=1}^M \int [X_j(t) - m_1 w_j(t - s_1; x_1, y_1)]^2 dt \quad (2)$$

is a minimum; M is the number of stations used in the analysis.

As the next step, the observed record $X(t)$ is replaced by the residual waveform, given by

$$X'_j(t) = X_j(t) - m_1 w_j(t - s_1; x_1, y_1) \quad (3)$$

and the second point source (m_2, s_2, x_2, y_2) is determined by the same procedure.

After N iterations—until no more significant decrease in error occurs—we obtain N point sources, (m_i, s_i, x_i, y_i) , with $i = 1, 2, \dots, N$, and the source time function can be calculated by

$$S(t) = \sum_{i=1}^N m_i u(t - s_i) \quad (4)$$

where $u(t)$ is the unit ramp function and m_i is the seismic moment of the i^{th} subevent. The final approximation error is given by

$$\Delta_N = \sum_{j=1}^M \int_0^\infty [X_j(t) - Y_j(t)]^2 dt = r_x(0) - r_w(0) \sum_{i=1}^N m_i^2 \quad (5)$$

which, when we use the normalized form to the zero-lag autocorrelation of the

observed seismograms, may be written as

$$\bar{\Delta}_N = 1 - \sum_{i=1}^N m_i^2 \sum_{j=1}^M r_{wj}(x_i, y_i) / r_{xj} \quad (6)$$

where $r_{wj}(x, y) = \int_0^\infty [w_j(t; x, y)]^2 dt$ and $r_{xj} = \int_0^\infty [X_j(t)]^2 dt$, and where r_x and r_w are autocorrelation functions of $r(t)$ and $w(t)$, respectively, N is the number of iterations, and M is the number of stations.

The resulting synthetic form $Y_j(t)$, the moment rate function $M_0(t)$, and the total seismic moment M_0 are given, respectively, by

$$Y_j(t) = \sum_{i=1}^N m_i w_j(t - s_i; x_i, y_i) \quad (7)$$

$$M_0(t) = \sum_{i=1}^N m_i u(t - s_i) \quad (8)$$

$$M_0 = \sum_{i=1}^N m_i \quad (9)$$

2. The Thessaloniki earthquake of June 20, 1978

On 20 June 1978 a moderate earthquake (O.T.20h, 03m, 21s, 40.7°N, 23.2°E, with $h = 3.5 \pm 4.1$ km, $M_b = 6.1$, $M_s = 6.4$; PDE) occurred in a valley located about 30 km east of the city of Thessaloniki in northern Greece; see Figure 1. This earthquake has been well studied by many investigators. CARVER and BOLLINGER (1979) suggested, from relocated aftershocks having an average depth of 8 km, that the fault plane dips northward at about 85°; MERCIER *et al.* (1979) found that in the investigated area reactivated faults striking 110° to 130° had sinistral normal motion, faults striking 60° to 90° had pure normal motion, and faults striking 60° to 45° had dextral normal motion. Properties of the Serbomacedonian geological massive are described by COMNINAKIS and PAPAACHOS (1979).

Fault-plane solutions based upon short-period and long-period data are given by PAPAACHOS *et al.* (1979a, 1979b). SOUFLERIS and STEWART (1980) studied the source process of this earthquake on the basis of trial-and-error waveform modeling of teleseismic, long-period body waves. They obtained a mechanism characterized by normal, left-lateral motion on a fault plane striking 283° and dipping 42°N. They also found that synthetics for an 8-sec trapezoidal time function (4 sec of duration, 2 sec of rise and fall time) at a source depth of 6 ± 2 km provided the best solution. The complexity of this multiple event, however, could not be resolved.

BARKER and LANGSTON (1981), utilizing the moment tensor formalism to teleseismic P and SH waves, obtained a north-trending tension axis and a nearly vertical compression axis with the following double-couple source parameters: strike

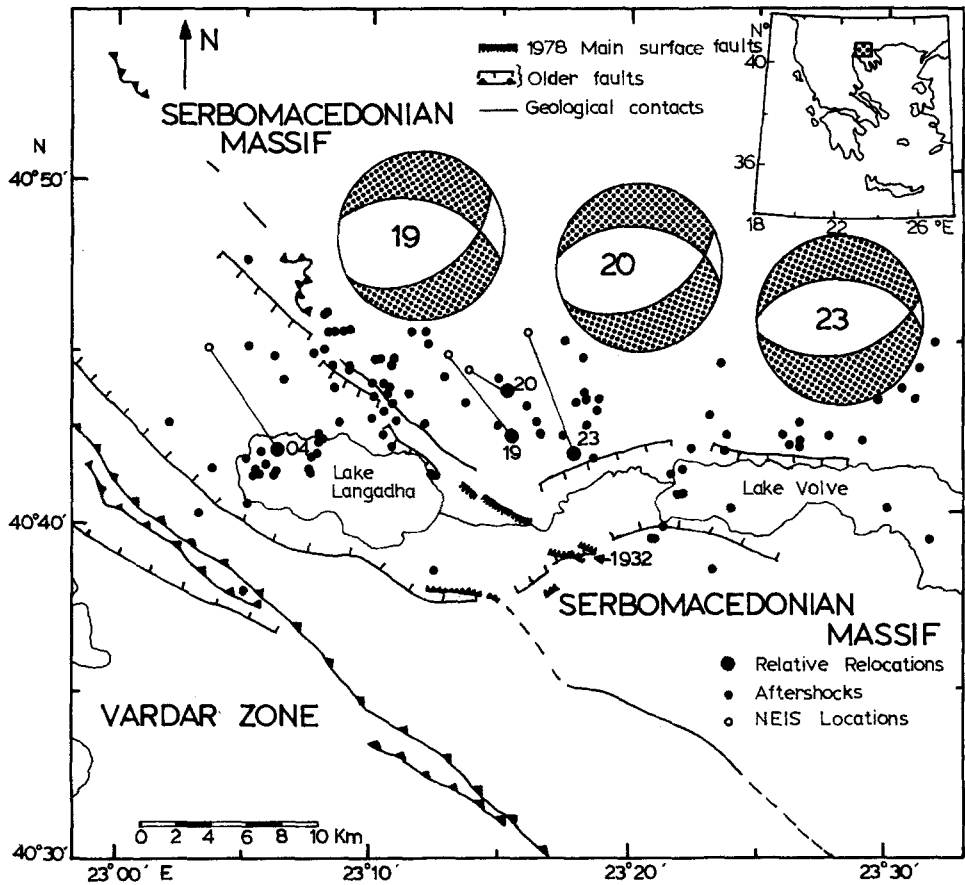


Figure 1

Tectonic setting of the 1978 Thessaloniki earthquake sequence. Faults and major geological contacts are from KOCKEL and MOLLAT (1977). Final USGS epicentres are connected to the final relocations of the same events. Surface ruptures which appeared during the mainshock and are likely to be of tectonic origin shown with heavy hatched lines on the down-thrown side. Preliminary locations for aftershocks, recorded by an array of portable stations, are shown as small solid circles. A fault segment active in 1932 and reactivated in 1978 is marked '1932'. Taken from SOUFLERIS and STEWART, 1981).

$280^{\circ} \pm 7^{\circ}$, dip $55^{\circ} \pm 3^{\circ}$, rate $-65^{\circ} \pm 5^{\circ}$, seismic moment 5.7 ± 10^{25} dyn-cm, and a skewed, triangular source time function with a rise time of about 1 sec and a duration of 6 to 8 sec. MALEY *et al.* (1979), on the basis of accelerograph records, suggest that the Thessaloniki earthquake was a complex rupture consisting of two or more events.

The intent of this paper is to verify this event and to obtain more information about the rupture and the distribution of asperities or barriers on the fault plane.

Table 1
Characteristics of the stations used

Sta. code	Magnif.	Azim. deg.	Back Azim., deg.	Epicentr. dist., deg.	Emerg. angle, deg.	Geom. factor	Atten. factor, T/Q
MAT	3000	47.30	316.17	82.41	17.1	624	1.167
SJG	700	283.53	50.76	77.84	18.2	412	1.157
AAM	1500	312.55	48.94	73.92	19.3	423	1.176
BAG	3000	72.84	311.04	84.74	16.5	402	1.469
BLA	1500	306.76	49.61	75.24	18.7	488	1.164
CAR	3000	278.09	49.68	83.28	16.9	434	1.182
CDH	1500	332.24	84.62	47.76	26.4	622	1.426
COL	1500	356.05	7.06	74.09	19.2	530	1.175
OGD	1500	307.10	53.23	69.45	20.4	516	1.198

3. Data analysis and results

Nine selected long-period seismograms recorded at WWSSN stations are used in the epicentral distance range 45° to 85° for minimizing complications due to upper mantle structure and core effects. At ranges greater than 80° the PcP phase arrives very close to the direct P, and it may affect the waveform. Only three stations between 80° to 85° were modelled successfully, however, without accounting for the PcP arrival. The characteristics of the stations used in the analysis are summarized in Table 1. From the Jeffreys-Bullen model of the Earth structure, the ray parameter,

$$P = \sin i_h / V_{ph} = \sin i_o / V_{p0} \quad (10)$$

is calculated for each one of the ten stations used; here i_h and i_o are the emergent and incident angles and V_{ph} and V_{p0} are the P-wave velocities at the source and the surface, respectively.

The effect of anelastic attenuation is taken into account by means of the Q operator of FUTTERMAN (1962), parameterized by the quantity T/Q_{av} (travel time divided by the average Q along the path). In this study a value of $T/Q_{av} = 1.0$ is considered valid for P-wave analysis, but, for epicentral distances greater than 80° , T/Q_{av} is no longer constant but increases rapidly up to 3.0 or even more and diffraction effects around the core would be involved.

Since the fault geometry of this event is known, we fix it in our inversion with a strike of 278° , and a dip angle of -70° (SOUFLERIS and STEWART, 1981); see Figure 1).

The inferred fault length of 35 km from the aftershock distribution (SOUFLERIS and STEWART, 1981, CARVER and BOLLINGER, 1981) is divided into 8 discrete points in the strike direction with a spacing of 5 km, and the fault width of 12 km is divided into 4 discrete points in the dip direction with a spacing of 4 km, so as to prepare synthetic wavelets from unit point sources at all possible source locations. Using $V_p = 6.0$ km/sec and $\rho = 2.8$ g/cm³, and placing a double-couple point source at

a depth of 8 km in a homogeneous half-space, we deconvolved the ten observational seismograms into a sequence of subevents:

$$(m_i, s_i, x_i, y_i), \quad i = 1, 2, \dots, 32$$

The deconvolution was repeated with 25 iterations for several combinations of rise and process (rupture) time in the least-squares sense. The best solution was obtained with a rise time of 2 sec and a process time of 5 sec; see Figure 2). The inferred source time function and the moment rate function

$$\dot{M}_0(t) = MT(t; \tau, t_c)$$

are plotted in Figure 3, where M_0 is the seismic moment and $T(t; \tau, t_c)$ is the source time function. From their shape we can recognize that the initial rupture is followed by a quiescence, which lasts about 8 to 10 sec, and after this is followed by 6 or 8 significant subevents.

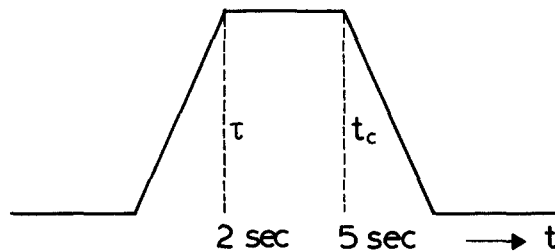


Figure 2
Source time function of the Thessaloniki earthquake of June 20, 1978.

We identify subevents 1, 2 and 3 as marked in Figure 3a. From the shape of the moment rate function we can recognize that the initial rupture is followed by a quiescence, which lasts 8 to 10 sec, and after this is followed by 6 or 8 significant subevents. We conclude that subevent 1, 2 and 3 represent the real source complexity. MALEY *et al.* (1979) suggest, on the basis of accelerograph records, that the Thessaloniki earthquake was a complex rupture consisting of two or more events, which are well resolved in our analysis.

The spatial distribution of the individual subevents on the fault plane, as obtained by the inversion analysis, is shown in Figure 4. We tried inversions while changing the point of the rupture initiation, although it may be inferred from the first arrival of P waves. A reasonably good fit between the synthetic and observed waveforms is obtained for the case in which the rupture initiates from the point with coordinates (5, 4), as shown in Figure 4. The dimension of the squares is proportional to the seismic moment corresponding to each subevent.

Table 2 gives the onset time s , the relative locations (x, y) , the moment rate function $\dot{M}_0(t)$, and the seismic moment M_{0i} of each individual shock, and also the

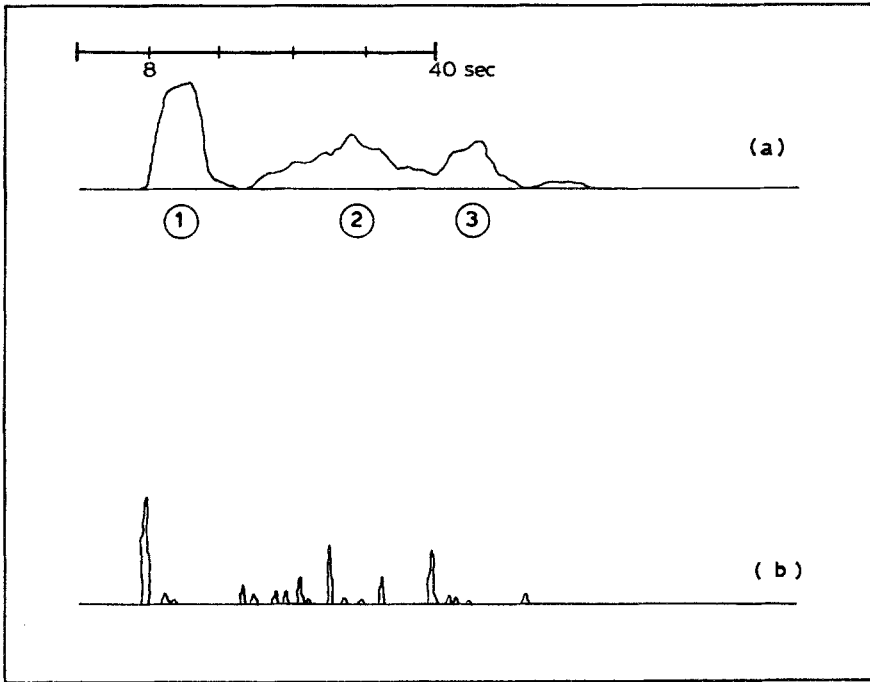


Figure 3
Far-field-displacement source time function (a), as obtained after 25 iterations and moment rate function (b).

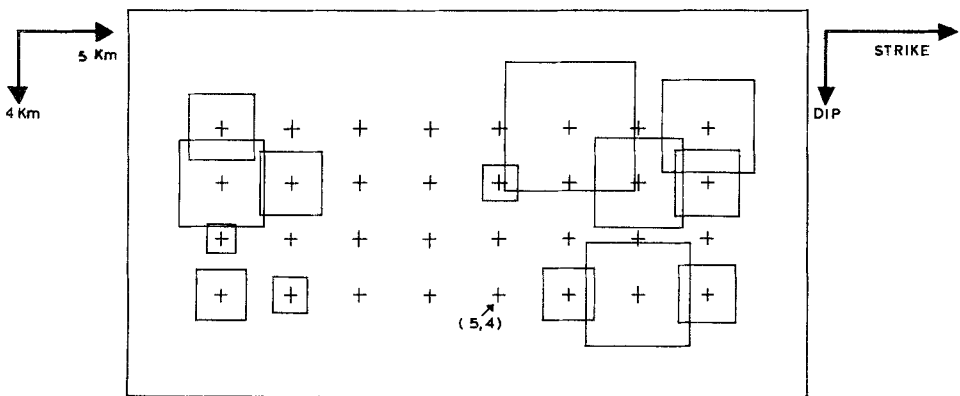


Figure 4
Spatial distribution of the individual subevents on the fault plane, as obtained by the inversion method.

Table 2
Subevent sequence of the fault plane as obtained by the inversion method

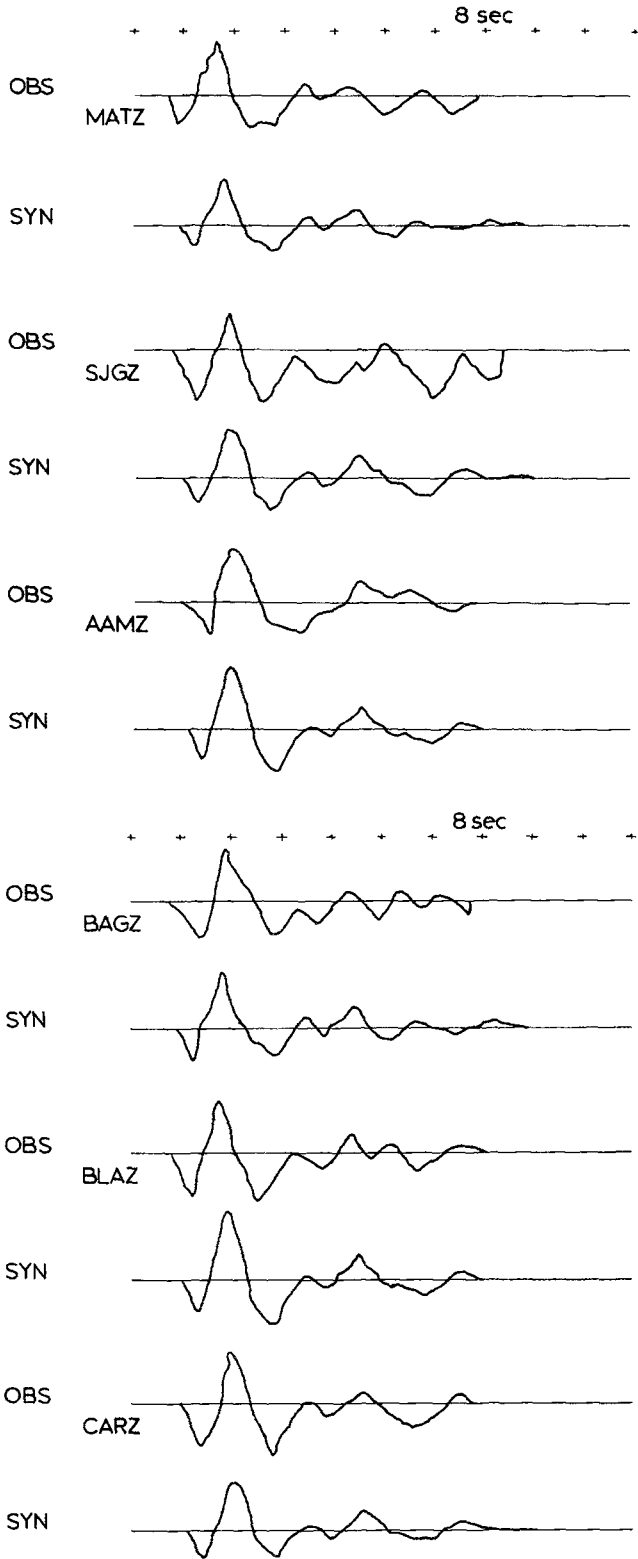
T , sec	x , km	y , km	No rate	M_0
1.6	10.0	0.0	0.9674E - 01	0.4837E + 00
2.0	5.0	-12.0	0.3087E - 01	0.1543E + 00
2.0	5.0	-12.0	0.1051E - 01	0.5253E - 01
4.0	15.0	-8.0	0.9223E - 01	0.4611E + 00
7.2	-20.0	0.0	0.5653E - 0.2	0.2827E - 01
8.0	15.0	-12.0	0.3218E - 01	0.1609E + 00
12.4	10.0	-4.0	0.1317E - 01	0.6586E - 01
14.4	15.0	0.0	0.1399E - 01	0.6997E - 01
17.2	5.0	0.0	0.7988E - 02	0.3994E - 01
19.2	-20.0	-8.0	0.5735E - 01	0.2867E + 00
21.6	-20.0	-4.0	0.1034E - 01	0.5172E - 01
21.6	5.0	-12.0	0.1892E - 01	0.9458E - 01
22.0	10.0	-4.0	0.4031E - 01	0.2016E + 00
24.8	15.0	-8.0	0.1676E - 01	0.8382E - 01
27.6	-20.0	-12.0	0.2451E - 01	0.1248E + 00
29.2	-15.0	-12.0	0.4535E - 01	0.2268E + 00
32.0	5.0	-12.0	0.1441E - 01	0.7206E - 01
32.8	5.0	-12.0	0.1776E - 01	0.8879E - 01
34.8	15.0	-12.0	0.2151E - 01	0.1075 E+ 00
36.4	15.0	-12.0	0.1380E - 01	0.6898E - 01
36.8	-20.0	-4.0	0.1465E - 01	0.7323E - 01
37.6	15.0	-12.0	0.1654E - 01	0.8269E - 01
39.6	-20.0	-12.0	0.1735E - 01	0.8673E - 01
41.2	-20.0	-12.0	0.1421E - 01	0.7104E - 01
44.6	15.0	-8.0	0.1898E - 01	0.9489E - 01
Total Seismic moment: 0.3332E + 01				

total seismic moment M_0 of the multiple sequence, in E25 (GGS).

From the onset time s_i and the spatial distribution of the subevents it is clear that the rupture propagated northeastward during the first several seconds and, after a quiescence of about 8 to 10 sec, moved westward. In Figure 5 the synthetic seismograms are compared with the observed ones. The waveform matching is very good at all stations, with a final approximation error Δ_{25} of 27%. In the multistation analysis described above it was assumed that all subevents had the same time history and focal mechanism.

4. Discussion and conclusions

The primary concern of this paper was to study the rupture process of the Thessaloniki earthquake of June 20, 1978. For this purpose we analysed teleseismic long-period P waves, using an iterative-deconvolution technique which was developed by



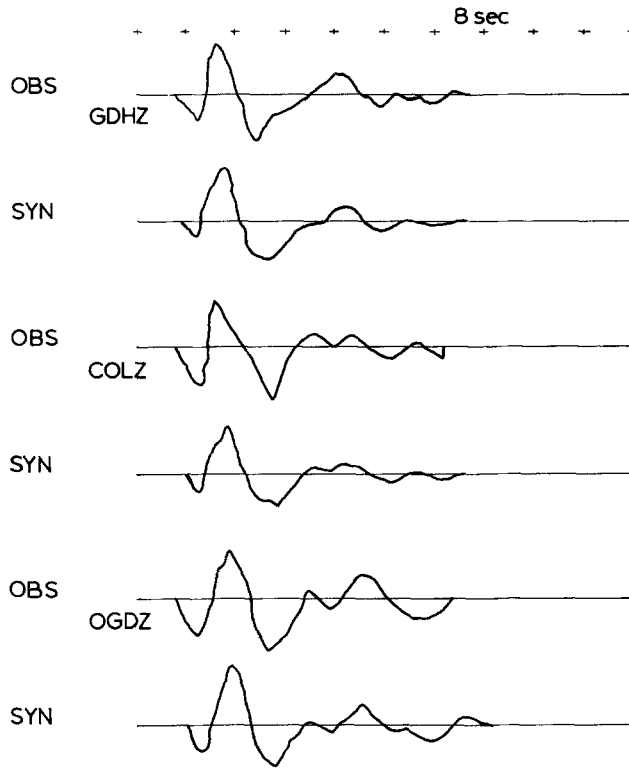


Figure 5
Observed and synthetic seismograms of the Thessaloniki earthquake of June 20, 1978.

KIKUCHI and KANAMORI (1982) and recently modified by KIKUCHI and SUDO (1984) and KIKUCHI and FUKAO (1985).

The distribution of the individual events on the fault plane may be interpreted in terms of a complex source model in which rupture starts at a small asperity and then triggers the larger-scale rupture of a neighbouring prestressed region which is difficult to break.

The far-field trapezoidal source time function used to model the point sources has an effective pulse width of 5 sec, which corresponds to a source dimension of about 10 km. The inferred source time function shows that the source process of the Thessaloniki earthquake was a complex event and included three significant sub-events with different moments, onset time, and relative location on the fault plane. The total duration of the time function is quite long for an earthquake of this size. For example, CIPAR (1980) modelled the Friuli earthquake ($M_s = 6.5$, $M_0 = 1.0 \times 10^{25}$ dyn-cm) with a time function of 4.5 sec, and STEWART and HELMBERGER (1981), the Bermuda earthquake ($M_s = 6.1$, $M_0 = 3.4 \times 10^{25}$ dyn-cm) with a time function of 3 sec.

The long duration and the low stress drop ($\Delta\sigma = 4$ bar), as estimated by SOUFLERIS and STEWART (1981), suggest an overall slow energy release during the Thessaloniki earthquake and may be due both to local reflections and to complexity of stress relaxation on the fault plane. Structural complexities near the source and along the propagation path are ignored, and the overall complexity of the observed waveforms is wholly attributed to the source complexity.

The summation of the seismic moments of all individual subevents amounts to 3.3×10^{25} dyn-cm, which is in a good agreement with the values obtained by SOUFLERIS and STEWART (1981) from body-wave analysis and by BARKER and LANGSTON (1981) from moment tensor inversion.

REFERENCES

- AKI, K. (1979), *Characterization of barriers on earthquake fault*. J. Geophys. Res. 84, 6140–6147.
- BARKER, S. J. and LANGSTON, C. A. (1981), *Inversion of teleseismic body waves for the moment tensor of the 1978 Thessaloniki, Greece, earthquake*. Bull. Seismol. Soc. Am. 71, 1423–1444.
- CARVER, D. and BOLLINGER, G. A. (1981), *Aftershocks of the June 20, 1978, Greece earthquake: A multimode faulting sequence*. Tectonophysics 73, 343–363.
- CIPAR, J. (1980), *Teleseismic observations of the 1970 Friuli earthquake sequence*. Bull. Seism. Soc. Am. 70, 963–983.
- COMNINAKIS, P. E. and PAPAZACHOS, B. C. (1979), *Distribution of macroseismic effects of the 1978 two major earthquakes in the Thessaloniki area of Northern Greece*, Public, N.11, Geophysical Laboratory, Aristoteleian University of Thessaloniki.
- FUTTERMAN, W. I. (1962), *Dispersive body waves*. J. Geophys. Res. 67, 5279–5291.
- KANAMORI, H. and STEWART, G. S. (1978), *Seismological aspects of the Guatemala earthquake of February 21, 1977*. J. Geophys. Res. 83, 3427–3434.
- KIKUCHI, M. and KANAMORI, H. (1982), *Inversion of complex waves*. Bull. Seismol. Soc. Am. 72, 491–506.
- KIKUCHI, M. and FUKAO, Y. (1985), *Iterative deconvolution of the complex body waves from great earthquakes: The Tokachi-Oki earthquake of 1968*. Phys. Earth Planet. Interiors 37, 235–248.
- KIKUCHI, H. and SUDO, K. (1984), *Inversion of teleseismic P-waves of the Izu-Oshima, Japan, earthquake of January 14, 1982*. J. Phys. Earth. 32, 161–171.
- KOCKEL, F. and MOLLAT, H. (1977), *Geologischen karte der Chelkidhiki und Angrenzender Gebiete, 1: 100,000* (Nord Griechenland).
- LAY, T. H., KANAMORI, H. and RUFF, L. (1982), *The aperiodicity and the nature of large subduction zone earthquakes*. Earthq. Prediction Res. 1, 3–71.
- MALEY, R. P., BUFE, C. G., YERKES, R. F., CARVER, D. C. and HENRISEY, R. (1979), *The May–July 1978 earthquake sequence near Thessaloniki, Greece*. U.S. Geol. Surv. Open-File Rept. 80–937.
- MERCIER, T. L., MOUYARIS, N., SIMEAKIS, C., RONDOYANNI, T. and ANGELDHIS, C. (1979), *Intra-plate deformation: A quantitative study of the faults activated by the 1978 Thessaloniki earthquakes*. Nature 278, 45–48.
- MIKUMO, T. and MIYATAKE, T. (1978), *Dynamic rupture process on a three-dimensional fault with non-uniform frictions, and near field seismic waves*. Geophys. J. R. Astr. Soc. 54, 417–438.
- PAPAZACHOS, B. C., MOUNDRAKIS, A., PSILOVIKOS, P. C. and LEVANTAKIS, G. (1979a), *Surface fault traces and fault plane solutions of the May–June 1978 shocks in the Thessaloniki area, North Greece*. Tectonophysics 53, 179–183.
- PAPAZACHOS, B. C., MOUNTRAKIS, A., PSILOVIKOS, P. C. and LEVENTAKIS, G. (1979b), *Focal properties of the 1978 earthquake in the Thessaloniki area*. Bulgarian Geophys. J. 6, 72–80.
- SOUFLERIS, C., JACKSON, J. A., KING, G. C. P., PAPAZACHOS, B. C., SCHOLZ, C. H., SPENCER, C. P. (1981),

- The Thessaloniki (N. Greece) 1975 earthquakes: A delayed multiple event sequence.* Geophys. J. R. Astr. Soc. 68, 429–458.
- SOUFLERIS, C. and STEWART, G. S. (1981), *A Source study of Thessaloniki (N. Greece) 1978 earthquake sequence.* Geophys. J. R. Astr. Soc. 67, 343–358.
- STEWART, G. S. and HELMBERGER, D. V. (1981), *The Bermuda earthquake of March 24, 1978: A significant oceanic intraplate event.* J. Geophys. Res. 86, 7027–7036.
- WYSS, M. and BRUNE, J. (1967), *The Alaska earthquake of 28 March 1964: A complex multiple rupture.* Bull. Seismol. Soc. Am. 57, 1017–1023.

(Received 16th December 1985, revised/accepted 25th July 1986)